Highly Water-Stable Rare Ternary Ag-Au-Se Nanocomposites as Long Blood Term X-rays Computed Tomography Contrast Agents

Carlos Caro,[a] Mariona Dalmases,[b,c] Albert Figuerola,[b,c] María Luisa García-Martín,[a,*] Manuel Pernia Leal [a,d,*]

[a]BIONAND, Andalusian Centre for Nanomedicine and Biotechnology (Junta de Andalucía-Universidad de Málaga), Málaga, Spain

[b]Departament de Química Inorgànica i Orgànica, Secció de Química Inorgànica, Universitat de Barcelona, Martí i Franquès 1-11, 08028 Barcelona, Spain

[c]Institut de Nanociència i Nanotecnologia (IN2UB), Universitat de Barcelona, Martí i Franquès 1-11, 08028 Barcelona, Spain

[d]Departamento de Química Orgánica y Farmacéutica, Universidad de Sevilla, 41012 Seville (Spain)

KEYWORDS: Constrast agents, computed tomography, ternary nanoparticles, Pegylation, molecular imaging.

ABSTRACT

X-ray computed tomography (CT) is a powerful and widely used medical non-invasive technique that requires intravenously administration of contrast agents to enhance the sensitivity and visualization of soft tissues. In this work, we have developed a novel CT contrast agent based on ternary Ag-Au-Se chalcogenide nanoparticles. A facile and gentle ligand exchange by using a 3 kDa PEGylated ligand with a dithiol dihydrolipoic as an anchor resulted in highly water-soluble and monodisperse nanoparticles. Moreover, the injected PEGylated ternary NPs presented excellent characteristics as a CT contrast agent

with high bioavailability, low cytotoxicity and long blood circulation times with slow uptake by the mononuclear phagocyte system, thus being ideal for *in vivo* imaging.

INTRODUCTION

Computed Tomography (CT) is one of the most commonly used medical imaging diagnostic techniques. This powerful non-invasive technique provides high spatial (3-D) and temporal resolution images, based on the attenuation of the X-ray intensity. Thus, CT is extensively used in certain tissues such as the cardiovascular system, the gastro-intestinal tract and the brain, especially for studies that require high speed in data acquisition, such as the visualization of cardiac motion. However, X-ray CT presents some intrinsic drawbacks such as low sensitivity, ionizing radiation, and limited contrast in soft tissues. Both sensitivity and contrast can be improved by using contrast agents, such as the iodine derivatives currently available for clinical applications. However, these contrast agents show important drawbacks, namely, short circulation times with rapid renal clearance, side toxicity effects due to the necessity of high doses, and inefficient X-ray attenuation with the consequent use of high energy X-rays. To overcome these limitations engineered nanoparticles based on elements with higher atomic number than iodine (Z = 53), like lanthanides, tantalum, bismuth and gold have been synthesized as novel CT contrast agents. Among these engineered CT contrast agents, gold-based nanoparticles have received considerable attention due to the low toxicity, higher X-ray attenuation, the ease to control the size, shape and morphology of the NP in the synthesis and the efficacy on the functionalization with thiolated derivates. Furthermore, prolonged blood circulation times and better bioavailability can be achieved by controlling other factors such as the organic coating or the outermost surface charge of the nanoparticles.

Recently, our research group has demonstrated that coating small NPs (~6 nm) with 3kDa PEG-OH molecules resulted in optimal stealth properties and increased blood circulation times, thus turning these NPs into potential contrast agents for molecular imaging or tumor targeting.

Herein, we report the synthesis of water soluble ternary Ag-Au-Se nanocomposites. Interestingly, this noble metal-based ternary chalcogenide system has been tested previously as a potential thermoelectric energy conversion material. (ref. Dalmases, M. et al. Chem. Mater. 2016, 28, 7017-7028) However, their applications in the field of biomedicine have not been explored yet. In addition to the presence of gold in the nanoparticle composition, the selenium could provide important functions as a reducing cancer agent, and silver could be utilized as a potential biosensor or anti-microbial agent, among others, thus giving to this chalcogenide system a high potential for biomedical applications. In this report, we explored the application of these rare Ag-Au-Se ternary nanostructures as novel X-ray computed tomography contrast agents. To achieve this aim, the ternary nanocomposites were transfered in aqueous medium by a simple ligand exchange functionalization. The use of a ligand with a dihydrolipoic acid (DHLA) anchor combined with a 3 kDa poly ethylene glycol (PEG) chain provided highly water-soluble stable rare ternary nanoparticles that exhibited excellent *in vitro* and *in vivo* properties as X-rays CT contrast agents with long blood circulation times.

RESULTS AND DISCUSSION

Ligand exchange protocol for the Ag_3AuSe_2 nanoparticles.

To render water-soluble rare Ag-Au-Se ternary nanoparticles, we designed a modular ligand DHLA-PEGn-OH that presents a dithiol terminal group to strongly anchor the nanoparticle surface and a PEGylated chain of 3 kDa to ensure the solubility in water, the

stability on different media, like physiological solution and plasma, and minimize plasma proteins adsorption to avoid a rapid clearance by the mononuclear phagocytic system (MPS). The ligand exchange occurs by a previous ring opening reduction of the disulfide LA-PEGn-OH to the more active form, dithiol DHLA-PEGn-OH. Then, a vigorous shaking of a toluene (or chloroform) solution of monodisperse rare Ag-Au-Se ternary nanoparticles, the corresponding PEGylated dithiol DHLA-PEGn-OH and triethylamine as a strong base, brought an effective cap exchange of the stabilizing surfactants onto the ternary nanoparticles. The PEGylated ternary nanoparticles were automatically transferred to the aqueous phase without perturbing the colloidal properties of the hybrid nanocomposites as shown in **Figure 1**. This step is the more critical aspect to take into consideration since the functionalization process and in particular the transfer of the nanoparticles in aqueous solution could bring the formation of agglomerates or uncontrolled aggregation with the consequent loss or modification of their properties. TEM images showed that the PEGylated nanoparticles kept the same colloidal distribution that the hydrophobic nanoparticles. Although the TEM images showed similar diameter sizes and a great colloidal stability, the hydrodynamic diameter sizes were also measured through Dynamic Light Scattering (DLS) to obtain a more complete information on the behavior of the bulk hybrid nanoparticle solution. The hydrophilic nanoparticles presented HD diameters of 30.6 and 25.4 nm in PBS and plasma respectively, thus indicating the absence of aggregates. Furthermore, the negative values measured in the Z-potential allow the nanoparticles to reduce uncontrolled aggregation in plasma, as shown in **Figure 2**. The presence of the dithiol PEGylated at the nanoparticle surface was also confirmed by different physico-chemical techniques such as FTIR, ^{1}H NMR and UV-Vis spectroscopies (**Figure 3**). The FTIR spectra before and after the functionalization are shown in **Figure 3a**. As can be observed, the spectrum of the

hydrophilic hybrid nanoparticle showed the presence of the main peaks of the DHLA-PEG-OH ligand: 1466 cm^{-1} (C-H bend vibration), 1359 cm^{-1} (C-H bend vibration), 1341 cm^{-1} (C-H bend vibration), 1307 cm^{-1} (anti-symmetric stretch vibration), 1268 cm^{-1} (C-O stretch vibration), 1238 cm^{-1} (C-O stretch vibration), 1092 cm^{-1} (C-O-C stretch vibration) and 942 cm^{-1} (CH out-of-plane bending vibration). In the same manner, the NMR analysis of the hydrophilic PEGylated nanoparticles resulted in a ^{1}H NMR spectrum practically identical to the DHLA-PEG-OH ligand (**Figure 3b**). UV-Vis analysis of the nanoparticles showed no significant changes before and after functionalization (Figure 3c). Ag_3AuSe_2 has been theoretically identified as a semiconductor with a band gap energy of ca. 0.2 eV. (ref. C. M. Fang et al. Journal of Physics and Chemistry of Solids, 63 (2002) 457-464) Such a small band gap would in principle be responsible for absorption of very low energy photons at the near infrared region, above 1000 nm, although this has never been experimentally reported yet. In both spectra, before and after functionalization, a weak and wide absorption band (or group of bands) between 500 and 700 nm can be observed. These bands could be assigned either to the intrinsic band structure of the ternary Ag_3AuSe_2 material, or to the Surface Plasmon Resonance (SPR) absorption band of a small population of metallic Au nanoparticles that might have been formed during the synthesis of the ternary Ag_3AuSe_2 nanostructures. In order to discern between the two hypotheses, powder X-ray diffraction measurements were performed to the sample before functionalization. The XRD spectrum does not show any band confirming the presence of metallic Au, but this could be due to both the low amount of Au nanoparticles and to their very small domain size. Thus, the origin of the 500-700 nm absorption band can not be unambiguously assigned to a Ag_3AuSe_2 intraband transition or simply to the presence of metallic Au impurities. After ligand exchange, the new absorption band below 450 nm can be assigned to the PEGylated ligand (**Figure 3c**, black). To quantify the amount of

ligand attached to the hybrid ternary nanoparticle, a thermo-gravimetric analysis (TGA) was performed, resulting that the 80% of the weight corresponds to the organic ligand (**Figure 3d**). It is worth mentioning that before performing all these experiments, a thorough purification process was done by filtering the solution in a centrifuge device with a MWCO 30kDa under centrifugation (4500 rpm for 20 min) till the filtered solution remained clean and free of excess ligand.

Cytotoxicity

After an exhaustive physical chemical characterization, the following step was the evaluation of the cellular biocompatibility of the PEGylated rare Ag-Au-Se ternary nanoparticles. Since, the presence of silver cations in the nanoparticles could lead to severe toxicity problems, the cytotoxicity of the hybrid nanoparticles was evaluated using the C6 rat glioma cell line as a working model. The cultured cells were exposed to increasing concentration of the PEGylated rare Ag-Au-Se ternary nanoparticles from 0.5 μg/mL to 500 μg/mL for 24 h (**Figure 4a**), giving as result 100% of cell viability even at the high concentration of 50 μg/mL, with a calculated LD_{50} of 296 μg/mL (**Figure 4b**). This means that the PEGylation onto the ternary nanoparticles protects the inorganic surface from the external medium avoiding possible leaching of cations from the inorganic nanoparticle. These results support the great potential of these rare Ag-Au-Se nanoparticles in biomedical applications, as reported below in the following section.

***In vivo* studies**

After the *in vitro* characterization of the PEGylated rare ternary nanoparticles, we performed *in vivo* studies of biodistribution and the bioavailability of these metal NPs to evaluate their potential as Computed Tomography contrast agents. Thus, after the inoculation in the tail vein of 10 mg of NPs per kg of balb/c mouse, we followed and

quantified by CT the *in vivo* accumulation of the injected nanoparticles in different organs at 1, 24, 48, 72 and 168 h (**Figure 5**). It was clearly observed an increase of the contrast after 1 h in liver and bladder, with ΔHounsfield units of 5.5 ± 1.5 and 5.2 ± 0.7 respectively. In addition, postmortem quantification of silver by ICP-MS in different organs at one hour after injection confirmed the accumulation of PEGylated NPs preferentially in liver and spleen (**Figure SX**). The concentration of NPs in the liver was maximal at 24 h, with ΔHounsfield units of 9.1 ± 0.5, and were totally excreted, i.e. contrast returned to basal values, at 168 h. The presence of metal NPs in the bladder, which is governed by a glomerular filtration limit of 6-8 nm, could be explained by shrinkage or partial degradation of the organic coating on the NPs as already described by our group (ref.). In fact, the bladder showed maximal contrast at 24 h (ΔHounsfield units of 15.7 ± 1.5), which support the idea of a slow filtration rate following a degradation process. Thus, to demonstrate the partial excretion of NPs through the kidneys, urine was collected during the first 24 h after the intravenous injection of the PEGylated NPs. The collected urine was purified through centrifugal filters and analyzed by TEM, EDX and UV-Vis (**Figure 6**). TEM and EDX analysis showed the presence of the ternary NPs in urine (**Figure 6a**). On the other hand, the UV-Vis spectrum revealed the presence of the absorption band characteristic of the inorganic sample (**Figure 6b**). As for the kidneys, no accumulation was observed at any time, as expected for these NPs, since their hydrodynamic (HD) diameters are in the range of 25.4 ± 0.7 nm in plasma, which, as previously reported (ref.), falls below the size for effective retention in the corpuscles of the kidney cortex. Moreover, to determine the lifetime of the circulating PEGylated NPs in the bloodstream, samples of blood plasma were analyzed at 1 and 24 h by TEM, EDX, UV-Vis and CT (**Figure 7**). The *ex vivo* analysis of plasma by CT showed an increase of contrast of 3.7 and 0.3 in Hounsfield units at 1 and 24 h,

respectively (**Figure 7a**). The UV-Vis spectrum of the plasma showed the presence of the absorption band of the inorganic NPs (**Figure 7b**), and the TEM and EDX analyses confirmed the presence of the rare ternary NPs in plasma at both experimental times (**Figure 7c** and **7d**). Thus, NPs showed high concentration in the bloodstream at one hour after injection and were still present at 24 h, although at very low concentration, indicating that NPs are being efficiently cleared out from the bloodstream at this time point, which is in good agreement with high concentrations found in liver and bladder. Finally, histology was performed on liver, kidneys and spleen (**Supplementary Fig. XX**) resulting no significant alterations in the tissues exposed to PEGylated metal NPs. These results confirm the long blood circulating times of the PEGylated rare ternary NPs, with partial renal clearance through urine and slow uptake by the mononuclear phagocyte system.

CONCLUSIONS

In summary, a novel X-ray computed tomography contrast agent based on a noble metal ternary chalcogenide Ag_3AuSe_2 was synthesized. The ternary Ag-Au-Se nanoparticles were transferred in water by a facile and fast ligand exchange method. The ligand molecule presents a dihydrolipoic acid as anchor group that binds strongly to the nanoparticle surface and a 3 kDa polyethylene glycol chain that allows the stabilization of the metal NPs in aqueous media giving excellent bioavailability and stealth properties. The functionalization of the ~8 nm inorganic core with the PEGylated dithiol DHLA-PEGn-OH ligand resulted a high stable mono-dispersed ternary NPs with a HD diameter of 25 nm in blood plasma. The PEGylated ternary NPs exhibited good contrast in computed tomography with low toxicity effects, and long blood circulation times with minimal mononuclear phagocyte system retention. This behavior is ideal for most clinical applications and it has great potential for *in vivo* molecular imaging.

EXPERIMENTAL SECTION

Chemicals

Reagents were obtained from commercial suppliers (Sigma Aldrich, Acros Organics, Fisher Scientific, Strem Chemicals and Rapp polymere) were used without further purification. Silver chloride (AgCl, 99.9%), selenium powder (Se, 99.99%), and tri-n-octylphosphine (TOP, 97%) were obtained from Strem Chemicals. Lipoic acid, Poly ethylene glycol 3000 Da, Triethylamine, Gold (III) chloride trihydrate ($HAuCl_4 \cdot 3H_2O$, ≥99.9%), tetraoctylammonium bromide (TOAB, 98%), tri-n-octylphosphine oxide (TOPO, 99%), Oleylamine (OLAm, 70%) were purchased from Sigma-Aldrich.

As solvents, Milli-Q water (18.2 MΩ, filtered with a filter pore size of 0.22 μM) from Millipore, toluene, isopropanol, ethanol, acetone, hexane, and anhydrous tetrahydrofuran were used (HPLC grade, Acros Organics). Purification of the water-soluble nanoparticles from free reagents was performed on centrifuge filters PALL with a molecular cut-off of 100 kDa (4000 rpm 20 min).

Methods

TEM images were obtained on a FEI Tecnai G2 Twin microscope operated at an accelerating voltage of 100 kV. TEM samples were prepared by dropping a solution of the corresponding metal nanoparticles at ~1 g/L of metal concentration on a carbon-coated copper grid and letting the solvent evaporate. The diameters were calculated on an average of hundred nanoparticles measured. The size distribution and zeta potential measurements of the dihydrolipoic acid derived metal nanoparticles were performed on a Zetasizer Nano ZS90 (Malvern, USA). The nanoparticles were dispersed in milli-Q water at a concentration of 50 mg/L of metal. The nanoparticles diameters were also measured in blood plasma by processing the animal blood after 1 hour of metal

nanoparticles injection. The measurements were done on a cell type: ZEN0118-low volume disposable sizing cuvette, setting 3.068 as refractive index with 173º Backscatter (NIBS default) as angle of detection. The measurement duration was set as automatic and three as the number of measurements. As analysis model general purpose (normal resolution) was chosen. Spectroscopy measurements in the range of visible radiation (800-400) and the near ultraviolet (400-300 nm) were obtained on a Cary 100 UV-Vis spectrophotometer (Agilent Technologies) with a light path of 1 cm. FTIR spectra were recorded with a FTIR-4100 Jasco using a single reflection ATR accessory (MIRacle ATR, PIKE Technologies) coupled to a liquid nitrogen cooled mercury cadmium telluride (MCT) detector. All spectra were recorded in the 4000 to 800 cm^{-1} range at 4 cm^{-1} resolution and accumulating 50 scans. Dihydrolipoic acid derived ligands were deposit as solid product and metal nanoparticles were prepared by dropcasting of a high concentrated nanoparticle solution onto a microscope slide (Thermo Scientific). The ^{1}H NMR spectra were recorded on a NMR Bruker Ascend™ 400 MHz spectrometer. The spectra were measured either in $CDCl_3$ or D_2O. Ag and Au concentrations were determined on an ICP-HRMS (ICP-HRMS, Element XR, Thermo Fisher). The metal nanoparticles were digested with aqua regia (a mixture of three parts of HNO_3 and one part of HCl). Briefly, to 25 µL of a solution of nanoparticles were added 2.5 mL of aqua regia in a volumetric flask. The mixture was left overnight. Then, milli-Q water was added to complete the total volume of 25 mL. Thermogravimetric analysis (TGA) was carried out by using a METTLER TOLEDO model TGA/DSC 1 in the temperature range of 30-800 °C at a heating rate of 10 °C min^{-1} under a N_2 flow (50 mL min^{-1}).

Synthesis of Rare Ternary Ag-Au-Se Nanostructures.

The formation of ternary NPs takes place by the reaction of the pre-synthesized Ag_2Se binary NPs with a Au(III) stock solution, as previously reported by some of us. (ref. Dalmases, M. et al. Chem. Mater. 2016, 28, 7017-7028)

The synthesis of the Ag_2Se precursor NPs was adapted from that published by Sahu and co-workers. (ref. Sahu, A.; Khare, A.; Deng, D. D.; Norris, D. J. Quantum Confinement in Silver Selenide Semiconductor Nanocrystals. Chem. Commun. 2012, 48, 5458−5460.) Briefly, 7.8 g TOPO and 6.6 mL oleylamine were degassed under vacuum at 120º C for 30 minutes. Meanwhile, two precursor solutions were prepared in the glovebox: 474 mg (6 mmol) Se were dissolved in 6 mL TOP and 572 mg (4 mmol) AgCl were dissolved in 4 mL TOP. Under N_2 atmosphere, the temperature was raised to 180º C and the TOP/Se solution was injected. Once the temperature was recovered the AgCl-TOP precursor solution was injected. After 20 minutes of reaction, the heating was stopped and the solution was let cool naturally. Once at 50º C, 5 mL of BuOH was added to the reaction flask to avoid solidification of the solvent. Finally, the solution was washed three times with EtOH, centrifuging 4 minutes at 4500 rpm and re-dispersing with 4 mL toluene. In this point, the Ag_2Se NPs were used as precursor to synthesize Ag_3AuSe_2 ternary nanoparticles, following our previously published protocol. (ref. Dalmases, M. et al. Chem. Mater. 2016, 28, 7017-7028) A gold ion solution in toluene was prepared via phase transfer of Au(III) ions from water to toluene, by using TOAB as a phase transfer agent. At this point, 180 μL of Ag_2Se NPs solution (3.6 μM) were mixed with 2 mL of a 6 mM Au(III)-TOAB stock solution in toluene and shaken for 1 h. Then, the final solution was washed once with EtOH and the NPs re-dispersed in toluene.

Synthesis of Di-Hydro Lipoic acid-PEGn-OH.

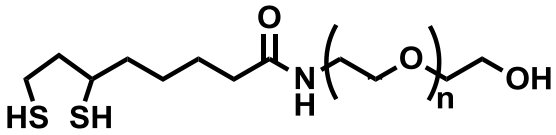

LA-PEGn-OH was prepared using a modified literature procedure. In brief, poly ethylene glycol (Mw: 3000 g/mol, 1 mmol, 3.0 g), (±)-α-lipoic acid (0.206 g, 1 mmol), and DMAP (0.012 g, 0.1 mmol) were dissolved in 100 mL of tetrahydrofuran and 10 mL of dichloromethane in a round-bottom flask at 0ºC under nitrogen atmosphere. Afterwards, a solution of dicyclohexyl carbodiimide (Mw: 206 g/mol, 5 mmol, 1 g) was added dropwise. The mixture was stirred at 0ºC for one hour and then left at room temperature overnight. The reaction mixture was filtered through a filter paper and solvents were rota-evaporated. The resulting oil was dissolved in 200 mL of chloroform and washed three times with HCl 1M (50 mL), $NaHCO_3$ concentrated (50 mL) and brine (50 mL), dried over $MgSO_4$, and filtered. After removing the volatiles under vacuum, flash chromatography on silica gel with CH_2Cl_2/MeOH (20:1) yielded 1.8 g (56%). Finally, to open the disulfide bond, LA-PEGn-OH (1.8 g, 0.56 mmol) in 10 mL of ethanol was added dropwise at 0ºC a solution of $NaBH_4$ (85 mg, 2.25 mmol) in 5 mL of H_2O. The mixture was stirred for 3 h at room temperature and the solvents were evaporated. The crude was dissolved in brine and the DHLA-PEGn-OH was extracted with $CHCl_2$, dried over $MgSO_4$, filtered and the volatiles evaporated under vacuum yielding the desired product quantitatively. ^{1}H NMR spectroscopy confirmed the desired product DHLA-PEGn-OH. ^{1}H NMR was in agreement with the reported data. ^{1}H NMR (400 MHz, $CDCl_3$): δ (ppm) 4.21-4.19 (m, 2H), 3.82-3.79 (m, 2H), 3.7-3.55 (m), 3.46-3.44 (m, 2H), 3.19-3.09 (m, 2H), 2.46-2.40 (m, 1H), 2.37 (t, *J* = 7.2 Hz, 2H), 1.96-1.88 (m, 1H), 1.83 (br s, 1H), 1.75-1.66 (m, 2H), 1.62-1.52 (m, 4H),1.42-1.34 (m, 2H), 1.29-1.21 (m, 2H), 1.10 (t, *J* = 7.1 Hz, 2H). FTIR peaks (cm^{-1}): 1466 (C-H bend vibration), 1359 (C-H bend vibration), 1341 (C-H bend vibration), 1307 (anti-symmetric stretch vibration), 1268 (C-O stretch

vibration), 1238 (C-O stretch vibration), 1092 (C-O-C stretch vibration), 942 (CH out-of-plane bending vibration).

Functionalization of metal nanoparticles (NPs)

The functionalization of the metal NPs were performed following the protocol previously published (ref.). Briefly, in a separating funnel was added a solution of 1.0 mL of ternary nanoparticles (10 g/L of metal), 1.0 mL of the corresponding dyhydrolipoic acid-PEGn-OH in a concentration of 0.1 M in $CHCl_3$ and 50 µL of triethylamine. The mixture was shaken gently and diluted with 5 mL of toluene, 5 mL of milli-Q water and 10 mL of acetone. Then, the ternary nanoparticles were transferred into the aqueous phase. After that, the aqueous phase was collected in a round-bottom flask and the residual organic solvents were rota-evaporated. Then, the dyhydrolipoic acid derived ternary NPs were purified in centrifuge filters with a molecular weight cut-off of 30 kDa, at 4500 rpm for 20 min. In each centrifugation, the functionalized ternary NPs were re-suspended with milli-Q water. The purification step was repeated several times until the filtered solution was clear. Then, the dyhydrolipoic acid derived ternary NPs were re-suspended in PBS buffer. Finally, to ensure high stable mono-dispersed ternary nanoparticles, the solution was centrifuged at 1500 rpm for 5 min.

Cytotoxicity assays.

C6 rat glioma cells were cultured in Dulbecco's Modified Eagle Medium (DMEM) supplemented with 2 mM L-glutamine, 10% fetal bovine serum (FBS) and 1% penicillin/streptomycin at 37º C in an incubator with a humidified atmosphere containing 5% CO_2. In order to perform the cytotoxicity assays, the C6 cells were plated at a density of 1 x 10^4 cells/well in a 96-well plate at 37ºC in 5% CO_2 atmosphere (200 µL per well, number of repetitions = 5). After 24 h of culture, the medium in the wells was replaced

with fresh medium containing the PEGylated ternary NPs in varying concentrations from 0.5 µg/mL to 500 µg/mL. After 24 h, the medium was removed, and 200 µL of fresh medium with MTT (0.5 mg/mL) was added to each well. After 2 h of incubation at 37ºC and 5% CO_2 the medium was removed and the formazan crystals were solubilized with 200 µL of DMSO, and the solution was vigorously mixed to dissolve the reacted dye. The absorbance of each well was read on a microplate reader (Dynatech MR7000 instruments) at 550 nm. The relative cell viability (%) and its error related to control wells containing cell culture medium without nanoparticles were calculated by the equations:

$$\boldsymbol{Relative\ Cell\ Viability\ (RCV)\ (\%)} = \frac{[\boldsymbol{Abs}]\boldsymbol{test}}{[\boldsymbol{Abs}]\boldsymbol{control}} \times \mathbf{100}$$

$$\boldsymbol{Error\ (\%)} = \mathbf{RCVtest} \times \sqrt{\left(\frac{[\boldsymbol{\sigma}]\mathbf{test}}{[\mathbf{Abs}]\mathbf{test}}\right)^{2} + \left(\frac{[\boldsymbol{\sigma}]\mathbf{control}}{[\mathbf{Abs}]\mathbf{control}}\right)^{2}}$$

where σ is the standard deviation.

***In vitro* and *in vivo* X-ray.**

In vivo mice experiments were performed in accordance with the ethical guidelines of Andalusian government. Male Balb/c mice (n = 3) with ca. 22 g in weight, provided by Janvier Labs were used. Animals were anesthetized with 1% isoflurane, the tail vein was cannulated and then the animals were placed in the X-Ray scanner. The functionalized nanoparticles were administered intravenously via tail vein at a concentration of 10 mg nanoparticles per kg.

The 2-D X-Ray images were acquired in a Bruker *in vivo* Xtreme multimodal imaging system with back-illuminated 4 mega-pixel camera (pixel dimensions 35 × 35 µm). The adquisition time was 1.2 seconds, the F-stop (aperture) was 1.4 and the X-ray energy was 45 kVp.

The CT images were acquired in a Bruker Albira small animal CT system. The X-ray Focal Spot Size (Nominal) used was 35 μm and the Energy used was 45 kVp, working at 400 μA. Values are Hounsfield units with the adjusted scale to see differences between soft tissues (leaving the bones overexposed) in 1000 images.

Histological analysis of the major organs

After one week post injection of the ternary NPs, the mice were sacrificed and the major organs were extracted. Histology of the major organs was determined by light microscopy. The tissues were fixed in 4% Formaldehyde (Panreac, pH 7 buffered) for 48 h, changing the 4% Formaldehyde after 24 h. Then, the samples were dehydrated through graded ethanol, and embedded in paraffin (temperature 56ºC for 2 h under stirring and vacuum). At this point, the Haematoxylin and Eosin stain was performed: Haematoxylin and Eosin (H&E): The paraffin-embedded samples were sectioned at 7 μm thickness and then were deparaffinized, rehydrated and stained with H&E, then dehydrated in ascending concentrations of ethanol, cleared in xylene and mounted in commercial glass slides.

ASSOCIATED CONTENT

Supporting Information. 2-D X-ray biodistribution, CT of heart, Histology of mouse and weight control of the animal. This material is available free of charge via the Internet at http://pubs.acs.org.

AUTHOR INFORMATION

Corresponding Author

*M.P.L.: email, mpernia@us.es

*M.L.G.M.: email, mlgarcia@bionand.es

Author Contributions

The manuscript was written through contributions of all authors. All authors have given approval to the final version of the manuscript.

Funding Sources

Financial support was provided by the Andalusian Ministry of Health (PI2013-0559 to MPL). MPL thanks to the Talentia Postdoctoral Fellowship Program (grant agreement 267226; Andalusian Knowledge Agency; Andalusian Regional Ministry of Economy, Innovation, Science and Employment) and to the V Plan Propio of the University of Seville for the Postdoctoral Fellowships. MD and AF acknowledge financial support from the Spanish MINECO through CTQ2015-68370-P, and from the Generalitat de Catalunya through 2014 SGR 129.

Notes

We thank the Nanoimaging Unit, Animal House facilities and the Histology Unit of Bionand and the SCAI-University of Malaga for the ICP measurements. We thank Dr. John R. Pearson and Dr. Juan Felix Lopez Tellez for useful discussions.

ABBREVIATIONS

CT, Computed Tomography; CA, Contrast Agents; TEM, Transmission Electron Microscopy; DLS, Dynamic Light Scaterring, Fourier Transform Infrared spectroscopy, FTIR; Surface Plasmon Resonance, SPR; Thermo-Gravimetric Analysis, TGA, Mononuclear Phagocytic System, MPS.

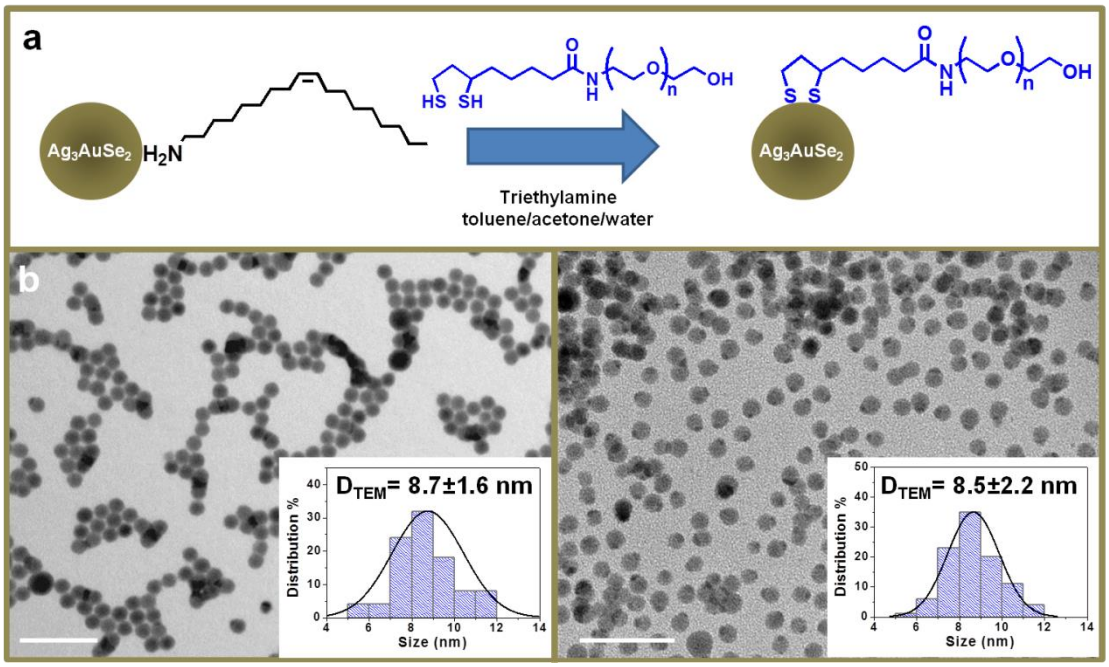

Figure 1. PEGylation of ternary Ag-Au-Se nanoparticles. (A) Scheme of the functionalization of lipoic acid-PEGn-OH nanoparticles. Representative TEM image of the NPs before (B) and after (C) functionalization with dyhydrolipoic acid-PEGn-OH. Scale bar corresponds to 50 nm. Insets correspond to histograms of the TEM diameters of the inorganic core measured on at least 100 nanoparticles.

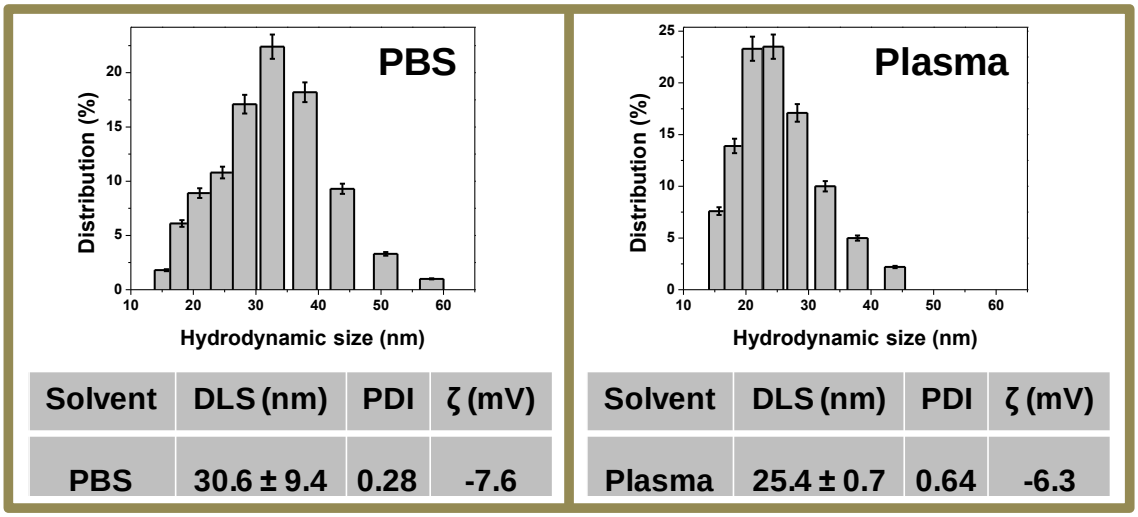

Solvent	DLS (nm)	PDI	ζ (mV)
PBS	30.6 ± 9.4	0.28	-7.6

Solvent	DLS (nm)	PDI	ζ (mV)
Plasma	25.4 ± 0.7	0.64	-6.3

Figure 2. Histogram of DLS sizes in PBS (left) and plama (right). Table of average hydrodynamic diameters, zeta potential of DHLA-PEGn-OH nanoparticles.

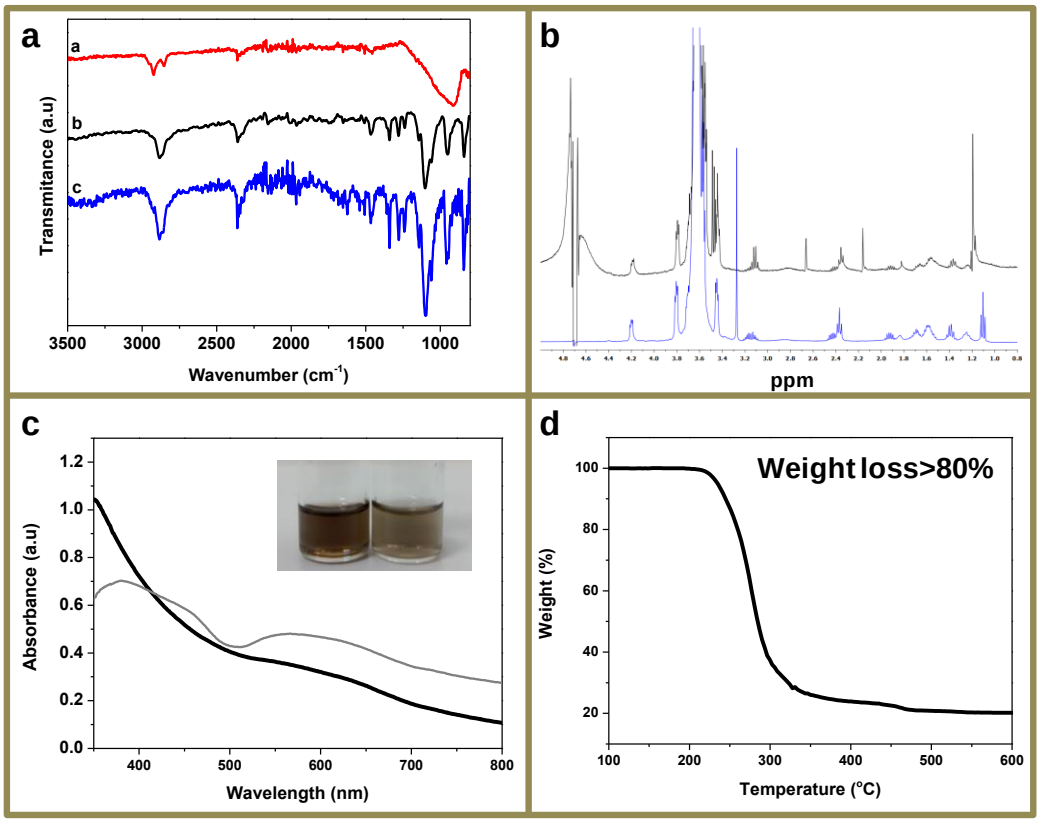

Figure 3. Characterization of PEGylated ternary Ag-Au-Se nanoparticles. (A) FTIR spectra of as-prepared ternary Ag-Au-Se NPs (a) and NP-DHLA-PEGn-OH (b) and ligand DHLA-PEGn-OH (c). (B) ^{1}H NMR spectra of ligand DHLA-PEGn-OH (blue) and NP-DHLA-PEGn-OH. (C) UV-vis spectra of the NP-DHLA-PEGn-OH showing a plasmonic abpsortion in the range between 500-700 nm (black) and NPs before ligand exchange process (grey). Images of the as-prepared ternary Ag-Au-Se NPs (left) and PEGylated Ag-Au-Se nanoparticles (right) functionalization. (D) Thermo-gravimetric analysis of the NP-DHLA-PEGn-OH.

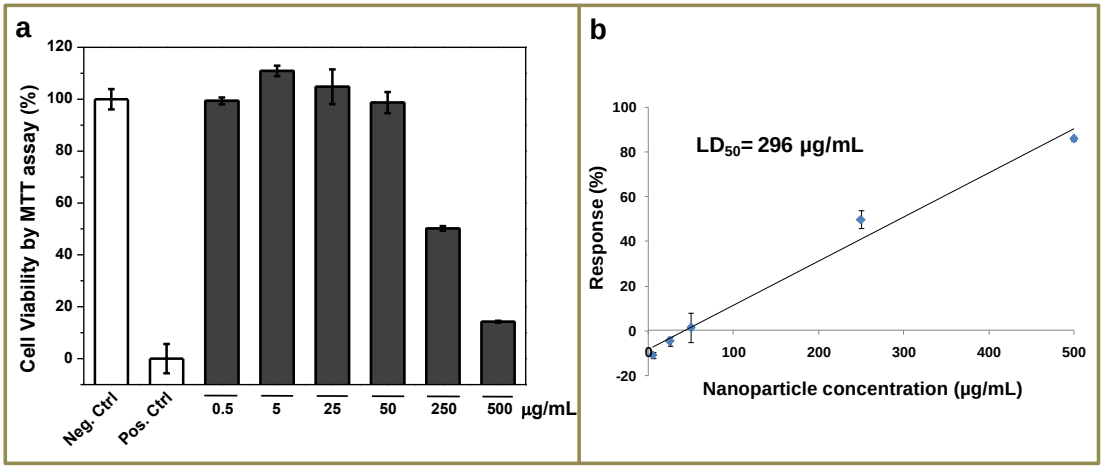

Figure 4. Cytotoxicity effects of PEGylated ternary Ag-Au-Se nanoparticles by the MTT assay of C6 cells treated for 24 h (A) at different concentrations. (B) Plot of cell death response over NP concentration.

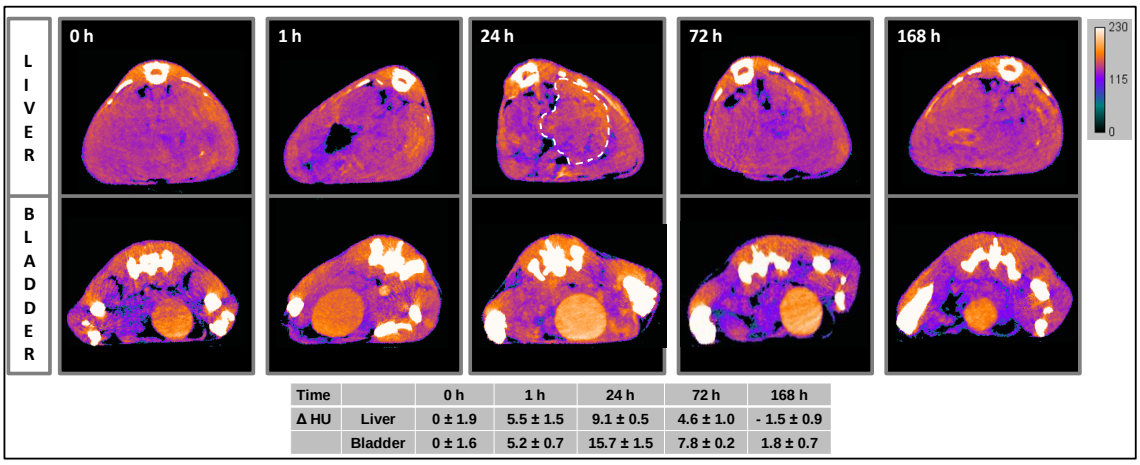

Time		0 h	1 h	24 h	72 h	168 h
Δ HU	Liver	0 ± 1.9	5.5 ± 1.5	9.1 ± 0.5	4.6 ± 1.0	- 1.5 ± 0.9
	Bladder	0 ± 1.6	5.2 ± 0.7	15.7 ± 1.5	7.8 ± 0.2	1.8 ± 0.7

Figure 5. Representative *in vivo* X-rays CT images at different experimental times after the intravenous injection of PEGylated ternary Ag-Au-Se nanoparticles. X-rays CT images of liver (Top) and bladder (Bottom) at 0, 1, 24, 72 and 168 h after nanoparticles injection. Values are Hounsfield units with the adjusted scale to see differences between soft tissues (leaving the bones overexposed). Table. Δ Hounsfield units values of liver and bladder at different times after intravenously injection of NPs. The average values were obtained by performing three experiments.

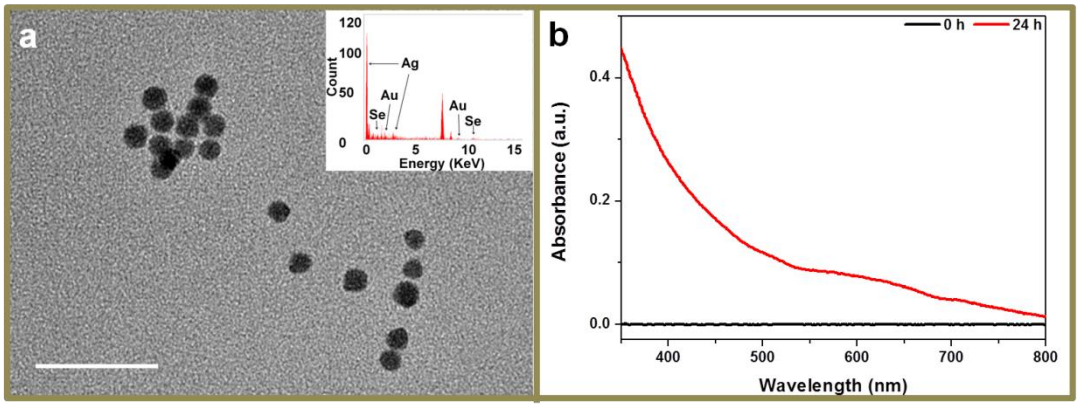

Figure 6. Analysis of excreted ternary Ag-Au-Se nanoparticles through the urine at 24 h after their intravenous injection. (A) Representative TEM image of NPs after purification and concentration by centrifugal PALL filter (MWCO: 30 kDa). Scale bar corresponds to 50 nm. (EDX spectrum of excreted 6 nm NPs). (B). UV-vis spectrum of the urine previously filtered and the spectrum was normalized with control urine.

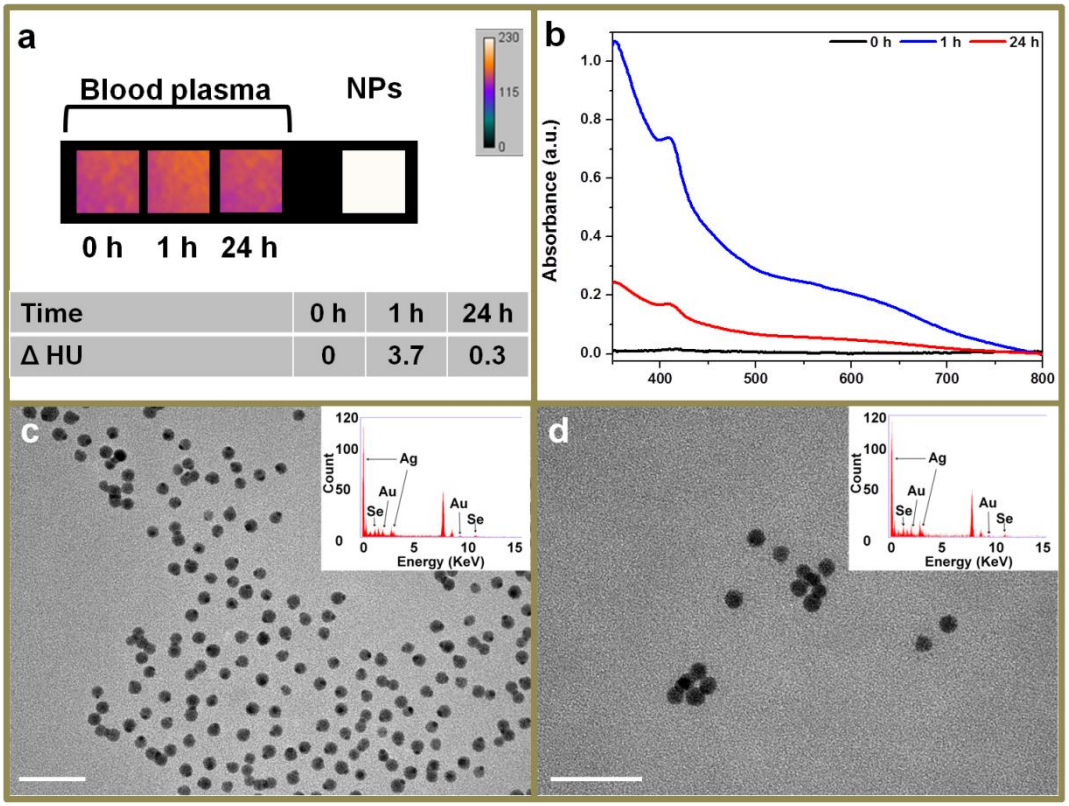

Figure 7. Analysis of blood plasma. (A) X-ray CT images of plasma at different experimental times (0, 1 and 24 h) after intravenously injection of ternary Ag-Au-Se nanoparticles and a solution of NPs before injection. Average values were obtained by performing three experiments. (B) UV-vis spectra of blood plasma at 0, 1 and 24 h after intravenously injection of NPs. Representative TEM image of extracted blood plasma at 1 h (C) and 24 h (D) after injection of NPs. Scale bars correspond to 50 nm.